TECHNICAL REPORT

nature neuroscience



# A hybrid approach to measuring electrical activity in genetically specified neurons

Baron Chanda[1,4], Rikard Blunck[1,4], Leonardo C Faria[2], Felix E Schweizer[3], Istvan Mody[2] & Francisco Bezanilla[1]

**The development of genetically encoded fluorescent voltage probes is essential to image electrical activity from neuronal populations. Previous green fluorescent protein (GFP)-based probes have had limited success in recording electrical activity of neurons because of their low sensitivity and poor temporal resolution. Here we describe a hybrid approach that combines a genetically encoded fluorescent probe (membrane-anchored enhanced GFP) with dipicrylamine, a synthetic voltage-sensing molecule that partitions into the plasma membrane. The movement of the synthetic voltage sensor is translated via fluorescence resonance energy transfer (FRET) into a large fluorescence signal (up to 34% change per 100 mV) with a fast response and recovery time (0.5 ms). Using this two-component approach, we were able to optically record action potentials from neuronal cell lines and trains of action potentials from primary cultured neurons. This hybrid approach may form the basis for a new generation of protein-based voltage probes.**

To understand the mechanisms underlying information processing by the central nervous system, it is necessary to track the activity of an ensemble of neurons. Although electrophysiological techniques remain the method of choice, they are unsuitable for recording from more than a few neurons at a time. Optical imaging using potentiometric and $Ca^{2+}$-sensitive dyes has been used to monitor electrical activity of neuronal populations with single-neuron resolution[1–4]. These dyes, unlike electrophysiological methods, have high spatial resolution in addition to high temporal resolution. As a result, activity even at the level of individual synapses can be imaged noninvasively[1,5]. Nevertheless, a significant limitation of the dye-based methods is the indiscriminate staining of both neuronal and non-neuronal cell types, which reduces the signal-to-background ratios considerably. Moreover, to dissect the circuit elements of a neuronal network, it is important to target the fluorescent probes to a genetically distinct class of neurons.

One particularly attractive approach is to use genetically encoded fluorescent probes to monitor neuronal activity[6,7]. To detect action potentials, a number of GFP-based sensors have been constructed by inserting a GFP molecule into various parts of voltage-gated $Na^+$ or $K^+$ channels. A reporter protein called FlaSH was generated by inserting the GFP into the C terminus of the S6 helix of the shaker $K^+$ channel[8], but the kinetics of the FlaSH response are quite slow, as they correlate mostly with C-type inactivation. In the SPARC protein, a GFP molecule was inserted between the linkers of domains I and II of the rat skeletal muscle $Na^+$ channel[9]. A third type of reporter protein termed VSFP1 was generated by attaching a cyan and a yellow fluorescent protein in tandem to a truncated $K^+$ channel[10]. Probes based on voltage-gated ion channels have some significant shortcomings. Voltage-gated ion channels undergo conformational changes over a narrow voltage range, which restricts the response range of these attached probes. In addition, these probes typically have modest fractional fluorescence changes since the GFP chromophore is buried within a beta barrel structure. Finally, many of these GFP-tagged, voltage-gated ion channels tend to be trapped in internal compartments, thereby increasing the background fluorescence.

A variety of two-component voltage sensors based on FRET have been described previously, from fixed fluorescent donors to translocating oxonol acceptors[11]. The measured fluorescence ratio changes vary from 34% per 100 mV ($\tau = 0.38$ ms) using fluorescent lectins[11] to 0.3% using transmembrane GFP (R.W. Friedrich *et al.*, *Soc. Neurosci. Abstr.*, 293.11, 1999). This technique successfully imaged activity from multiple individual neurons in leech nerve cords during locomotor activity, though to achieve dye penetration in this more intact preparation, a slower-translocating oxonol with a time constant of 0.4 s was used[12]. In comparison, the time constant of a widely used one-component dye like di-8-ANEPPS is about 2 μs at room temperature, with signals up to 22% per 100 mV[13,14].

In this paper, we describe a two-component system that is genetically encoded and enables the imaging of fast membrane potential changes in cells and neurons. This hybrid voltage sensor (hVOS) consists of a synthetic voltage-sensing molecule, dipicrylamine (DPA), and a genetically encoded fluorophore, farnesylated enhanced GFP (eGFP-F). DPA, which translocates from one side of the membrane to the other in response to potential changes, can also absorb energy from eGFP via FRET, even though it is nonfluorescent. Therefore, fluorescence from eGFP, which is attached to the inner leaflet of the plasma membrane through a farnesylation tag[15], becomes a genetically encoded optical readout for membrane potential changes. This hybrid approach gives a

[1]Departments of Physiology and Anesthesiology, [2]Department of Neurology and [3]Department of Neurobiology, David Geffen School of Medicine at the University of California Los Angeles (UCLA), Los Angeles, California 90095, USA. [4]These authors contributed equally to this work. Correspondence should be addressed to F.B. (fbezanil@ucla.edu).

Received 20 July; accepted 2 September; published online 2 October 2005; doi:10.1038/nn1558

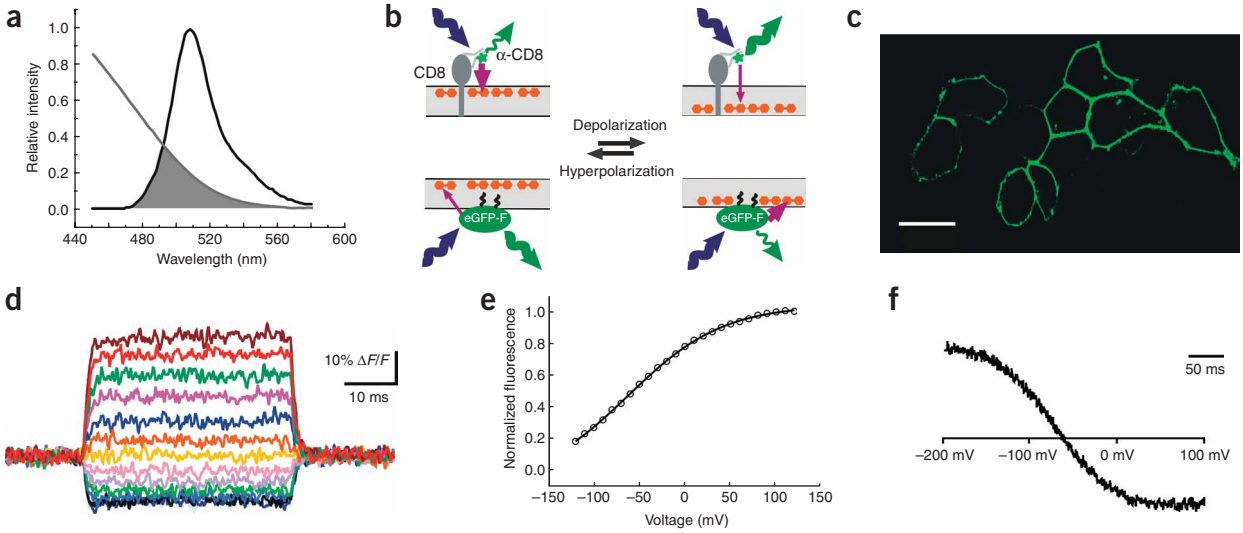


**Figure 1** The hVOS system in HEK 293 cells. (**a**) Overlap (shaded gray) of eGFP emission (black) and DPA absorption (light gray) leads to resonance energy transfer. (**b**) Upper panel, labeled anti-CD8 antibody bound to CD8 in the plasma membrane. In the hyperpolarized state, DPA molecules (orange dumbbell) accumulate on the outer leaflet of the membrane, dimming the fluorescence of antibody-bound dye as a result of FRET. Upon depolarization, translocation of DPA to the inner leaflet reduces FRET, which results in an increased dye fluorescence. Lower panel, eGFP-F molecules are anchored to the cytoplasmic face of the membrane. Hence, depolarization in the presence of acceptor DPA molecules quenches the eGFP fluorescence. (**c**) Confocal section of HEK293 cells expressing eGFP-F shows very little fluorescence from internal membranes. Scale bar, 20 μm. (**d**) Fluorescence response (shown as colored increments) of hVOS on voltage pulses from −120 to +120 mV in steps of 20 mV from a holding potential of 0 mV in patch-clamped HEK293 cells. These measurements, which are single sweeps, were carried out at room temperature in the presence of 6 μM DPA. (**e**) Normalized fluorescence voltage characteristic of hVOS in HEK293 cells. (**f**) Fluorescence response of hVOS in HEK293 cells on a voltage ramp from −200 mV to +100 mV (0.86 mV/ms).

large fractional fluorescence change (maximal $\Delta F/F$ = 34% per 100 mV) with a fast response time (time constant of 500 μs). We demonstrate that the hVOS probe can be used to measure trains of action potential spikes in primary neurons and is therefore a promising alternative to currently available probes for imaging neuronal activity.

## RESULTS

### A genetically encoded two-component system for voltage sensing

Our dual-component system for voltage sensing is based on changes in FRET between a synthetic voltage-sensing molecule and a genetically encoded fluorescent reporter. In our system, the voltage sensor is a charged hydrophobic molecule—DPA—that tends to partition into the lipid membrane close to the lipid water interface. DPA is a nonfluorescent absorber with an absorption maximum of 420 nm and has a significant spectral overlap with the emission of green fluorescent probes (**Fig. 1a**). DPA can therefore be excited through energy transfer by a green fluorescent label in close proximity; the calculated $R_0$ for an eGFP-DPA energy transfer pair is 37 Å. The extent of energy transfer for this pair can only be followed by measuring donor emission because DPA is fluorescently silent. Depending on the membrane potential, the negatively charged DPA molecules are distributed between the outer and inner leaflet of the plasma membrane. Changing the membrane potential results in rapid redistribution of DPA between the two membrane leaflets. This relocation changes the average distance between DPA molecules and an immobile reporter that is restricted to one leaflet of the membrane, thus changing the FRET efficiency. The effect on FRET for the two different reporter groups due to potential change is schematically shown in **Figure 1b**. The reporter moiety is a fluorescently labeled (Alexa-488) antibody to CD8. At resting membrane potential, most of the DPA molecules are closer to the outer leaflet of the membrane, so the emission of the antibody fluorophore is quenched. Upon depolarization, DPA molecules translocate from outside to inside with a time constant of several hundred microseconds. As a consequence, the distance between the antibody and the DPA increases, resulting in unquenching of the antibody fluorescence. Conversely, when the donor fluorophore is anchored to the inner leaflet, as with eGFP-F, depolarization results in quenching of donor fluorescence. eGFP-F was generated by fusing a 20-amino acid farnesylation sequence derived from c-Ha-Ras protein to the C-terminal end of eGFP. This sequence provides farnesylation and palmitoylation signals that target the host protein to the inner leaflet of the plasma membrane.

### hVOS signals are highly sensitive to voltage changes

In general, two-component systems, on which the hVOS is based, show a much higher sensitivity than the traditional potentiometric dyes, in which a single chromophore interacts with the membrane field. Since the hVOS is based on FRET changes between an immobile donor and a mobile acceptor, its sensitivity depends on the distance between the donor and the acceptor, as well as on their $R_0$, the distance of 50% transfer efficiency, which can be estimated from the spectral overlap (**Supplementary Note** online). We used eGFP-F, which is a known plasma membrane marker, as the immobile donor. A confocal section of HEK293 cells transfected with eGFP-F showed that most of the fluorescence was localized in the plasma membrane (**Fig. 1c**). The fluorescence was confined almost exclusively to the plasma membrane, with very little or no eGFP-F fluorescence from internal membranes. Under voltage-clamped conditions, single fluorescence sweeps of the hVOS system in HEK293 cells showed a large stepwise response (**Fig. 1d**). The maximum fractional fluorescence change ($\Delta F/F$) measured for a 100-mV pulse (from 0 to −100 mV) was 34%, making the measured fluorescence signal one of the largest among both fast and slow response dyes. Widely used potentiometric dyes, such as

**Table 1 Comparison chart of genetically encoded voltage sensors**

| | $\tau_{ON}$ (ms) | $\Delta F/F$ | Cutoff frequency | Dynamic range (mV) | | Basis |
|---|---|---|---|---|---|---|
| hVOS | 0.53 | 5–34% | 0.67 kHz | −150 | +50 | eGFP-F + DPA |
| FlaSH | 10.0 | 2.2%[a] | 0.02 kHz | −80 to +50 | −50 to +30 | Shaker-GFP/CFP |
| SPARC | 0.8–7 | 0.5% | ≥0.2 kHz | −80 | −10 | SkM1-GFP |
| VSFP1 | 0.7 | 1.8% | ? | <−140 | +200 | ΔKv2.1-YFP-CFP |

Shown are the characteristics of known genetically encoded fluorescent voltage sensing probes[9,10,30]. $\tau_{ON}$ gives the time constant of the fluorescence response to a step pulse. $\Delta F/F$ is the maximal normalized fluorescence change per 100 mV membrane potential change. Cutoff frequency indicates the corner frequency, up to which the system responds with 90% of the maximal change. The dynamic range marks the boundaries of the fluorescence response. The voltage sensors are based on constructs listed in the 'basis' column.
[a]This value was 5% for long depolarizations.

di-8-ANNEPS, which is used to follow fast potential changes, show fractional changes in the range of 5–20% per 100 mV in cells and hemispherical bilayers[14,16].

The steady-state fluorescence–voltage relationship could be fitted to a single Boltzmann curve with $V_{1/2} = -56.3$ mV and $z = 0.57$ (**Fig. 1e**). This is consistent with a two-state model in which the majority of the DPA molecules are distributed between the outer and the inner leaflet of the membrane. The apparent valence estimated from the Boltzmann fits of the fluorescence data was only 0.5 elementary charges, $e_0$, whereas the apparent valence from gating current measurements was approximately $1e_0$ (ref. 17). This is not unexpected, since the fluorescence response in FRET has a nonlinear dependence on distance. It is also likely that the charged group in the DPA molecule moves across the full extent of the electric field, whereas the larger chromophoric group moves across only a fraction of the electric field. The voltage dependence of the fluorescence change over the entire voltage range was evoked by a slow ramp between −200 mV to +100 mV (**Fig. 1f**). The fluorescence signals saturated at potentials below −180 mV and above +50 mV. Thus, the hVOS system has a large dynamic voltage range and has an almost linear response over the entire physiologically relevant voltage range.

## Speed and frequency response of the hVOS

In the neuron, an action potential is typically completed within a few milliseconds. To be able to follow this fast electrical activity, it is necessary for the reporter system to respond quickly and with high fidelity to changes in membrane potential. A monoexponential fit of the time course of fluorescence signal in response to a 100-mV voltage pulse gave a time constant of 0.54 ms (**Fig. 2a**). This is comparable to other voltage-sensitive reporter proteins such as VSFP1 ($\tau = 0.8$ ms) and SPARC ($\tau = 1.5$ ms), but much faster than FlaSH ($\tau = 10$–$20$ ms) (**Table 1**). The response speed of hVOS is rate-limited by the speed of the DPA moving through the plasma membrane and therefore may depend on membrane parameters like fluidity and lipid order. In squid axons, the speed of DPA translocation, estimated from gating current measurements, has been reported to be at least twofold faster than measured here[18]. Therefore, the speed of the response in the hVOS system may vary within certain bounds with different cell types and the physicochemical state of the membranes.

To test the ability of the dye system to follow trains of action potentials, we recorded the fluorescence response of hVOS by applying pulses of an amplitude (−60 to +40 mV) and duration (0.93 ms) matching those of a typical action potential with a varying interpulse interval (**Fig. 2b**). Our data indicate that shortening the interpulse interval to less than 1 ms attenuates the fluorescence signal. These data sets are plotted as a frequency response curve of hVOS (**Fig. 2c**). The cutoff frequency estimated by fitting the data was 667 Hz. For spike trains discharging at frequencies higher than 667 Hz, the amplitude diminished according to the fourth power of the input frequency. At frequencies higher than the cutoff, the hybrid voltage sensor will act as an integrator and the entire train will be detected as a single event. Even up to train frequencies of 750 Hz, the fluorescence still changed 90% of the maximal $\Delta F/F$ as an integrated event. In most excitable tissues, the trains of action potentials have maximal frequencies up to 250 Hz with action potential durations of 1–2 ms[19]. They should therefore be detectable by the hVOS system.

## Toxicity of hVOS

As DPA is a synthetic chromophore in the hVOS system, it is likely to have some phototoxicity[20]. In addition, it may have some intrinsic toxicity in neurons and brain slice preparations which may severely limit its use. We tested the phototoxicity of hVOS by repetitively pulsing the transfected HEK293 cells to a test potential in presence of DPA and while exposed to light. We used an increase in leak current as a measure of cell viability. In fluorescence recordings during cumulative exposure to light, the amplitude of the signal remained unchanged for

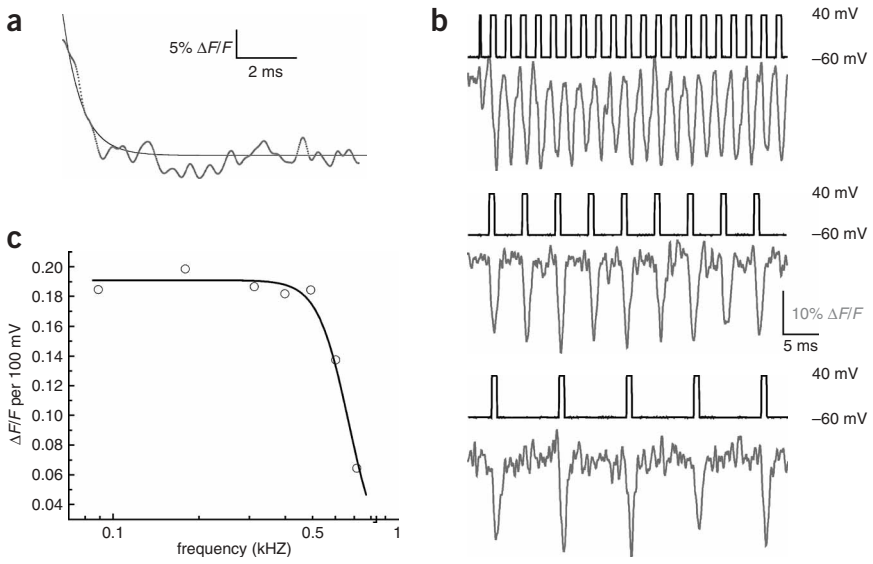


**Figure 2** Speed and recovery of hVOS. (**a**) Temporal resolution of hVOS as determined from fluorescence response (gray, noisy) to a voltage pulse from −60 mV to +40 mV in HEK293 cells. The trace was well fit to a monoexponential decay (black, smooth) and the $\Delta F/F$ was 20% per 100 mV for this cell in the presence of 6 μM DPA. All data shown in this figure are single sweeps. (**b**) Fluorescence response of hVOS (bottom, gray) to a train of voltage pulses (top, black) from −60 mV to +40 mV in HEK293 cells. The duration of the voltage pulses was 0.93 ms and the repetition frequencies were 416 Hz (top), 179 Hz (center) and 88 Hz (bottom). The data were filtered at 5 kHz. (**c**) Frequency response plot of hVOS obtained by varying the interpulse interval while keeping the pulse duration constant (0.93 ms).

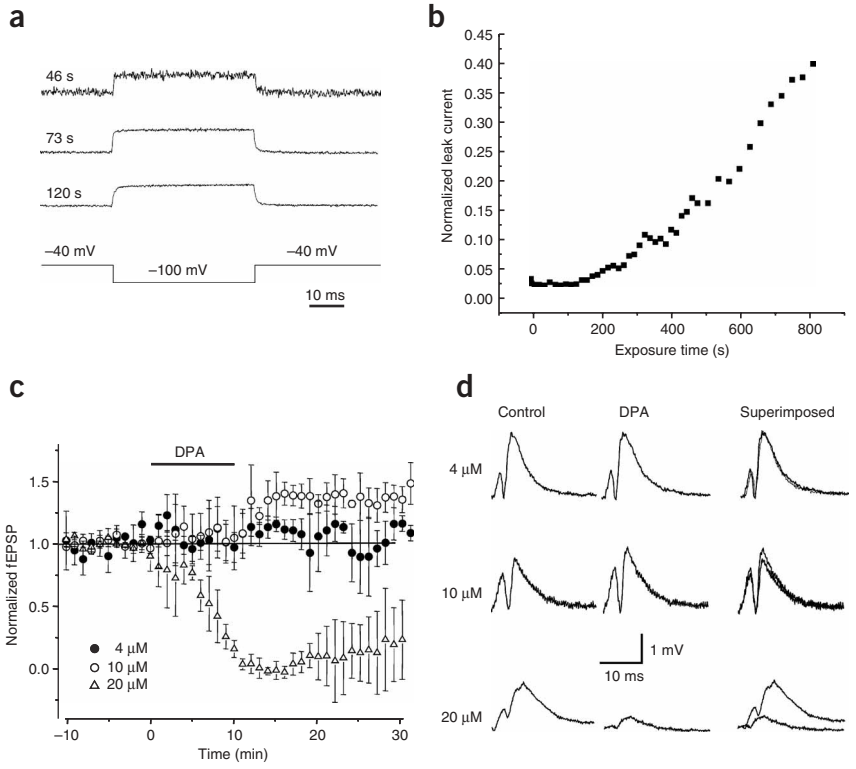


**Figure 3** Toxicity of hVOS system. (**a**,**b**) To test phototoxicity, we exposed HEK293 cells transfected with eGFP-F in the presence of DPA (>20 μM) with very high light intensities and determined the leak current as a measure of cell viability. In **a**, single sweeps of fluorescence response after different cumulative exposure are shown. Leak current with increasing excitation light exposure is shown in **b**. (**c**) Normalized CA1 field EPSP slope at the indicated DPA concentrations. The bar indicates the time DPA was added to the perfusion chamber. The values are normalized to the average slope of the fEPSPs recorded during the 10 min prior to DPA perfusion. Each concentration is shown as mean ± s.e.m. from 8 experiments carried out at 35 °C. (**d**) Effect of DPA on the shape of the population spikes recorded in the CA1 pyramidal cell layer. The traces depict population spikes evoked in a control ACSF and in the presence of the indicated concentration of DPA. The right panels show superposition of the two traces.

durations of up to 120 s of exposure (**Fig. 3a**). The plot of leak current versus cumulative light exposure shows very little phototoxic effect of DPA on cells for exposures of up to 100 s (**Fig. 3b**). Exposure beyond 200 s resulted in exponential reduction of cell viability, setting upper bounds for total light exposure.

Even if DPA is not significantly phototoxic, it is expected to increase the membrane capacitance, which may result in inhibition of action potentials. In addition, DPA is a charged hydrophobic ion and thus may have other toxic effects, either on action potentials or on synaptic transmission in live central neurons. We measured the amplitude of extracellularly recorded population spikes evoked by Schaffer collateral or commissural fiber stimulation in acute adult mouse hippocampal slices at 35 °C. The field EPSPs (fEPSPs) and population spikes were unaffected by 4 μM DPA, a concentration similar to that used for measurements in cultured cells (**Fig. 3c**,**d**). At 10 μM, DPA slightly enhanced the slope of the fEPSPs but left population spikes unaffected. A significant reduction in the evoked responses was observed when the DPA concentration was raised from 10 μM to 20 μM. This is consistent with reduced axonal excitability due to an increased capacitive load induced by high DPA concentrations. Thus, by keeping the concentration at or lower than 4 μM and the total light exposure to less than 200 s, we can minimize the side effects of DPA on neuronal recordings.

## Recording of action potentials in neurons

The ultimate test of an optical voltage reporting system is its ability to follow an action potential in neurons or neuronal cell lines. We initially transfected the neuronal cell line GT1 with eGFP-F[21]. A confocal section of GT1 cells transfected with eGFP-F and an overlay of all the sections are shown in **Figure 4a**,**b**. The eGFP-F was distributed mainly throughout the plasma membrane, although a significantly larger fraction of eGFP-F labeling is seen in the internal membranes in GT1 cell lines than in HEK293 cells. To stimulate action potentials in GT1 cells, the cells were depolarized to −50 mV by injecting a positive current to cells current-clamped at −90 mV (**Fig. 4c**,**d**). The time course of the measured fluorescence spike followed the time course of the action potential. The $\Delta F/F$ of the action potential (−48 mV → 10 mV) was 3% ($\Delta F/F = 5.2\%$ per 100 mV). For the measurement of action potentials, the DPA concentration was 2.2 μM instead of 6 μM

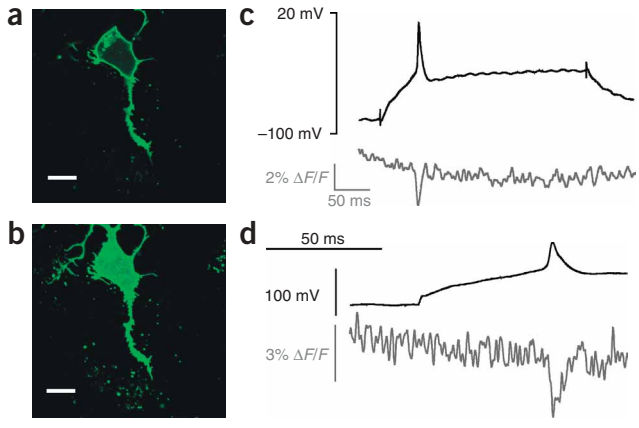


**Figure 4** Recording of action potentials with hVOS in GT1 cells. (**a**,**b**) Expression of eGFP-F in GT1 cells. (**a**) Confocal section of GT1 cells expressing eGFP-F. (**b**) Overlay of multiple confocal sections of cultured GT1 cells. Scale bars in **a**,**b**, 10 μm. (**c**,**d**) Fluorescence responses of hVOS on action potentials in GT1 cell culture in current-clamped cells measured at 32 °C with 2 μM of DPA. Cells were held at a resting potential of −100 mV and pulsed to −50 mV, where the action potential (black voltage trace) started to develop autonomously. The fluorescence response (gray trace) showed a normalized fluorescence change of 3% for 58 mV measured from the foot of the spike. The fluorescence trace was digitally filtered at 100 Hz after acquisition. (**d**) The trace was recorded with an expanded time resolution and digitally filtered at 200 Hz after acquisition.

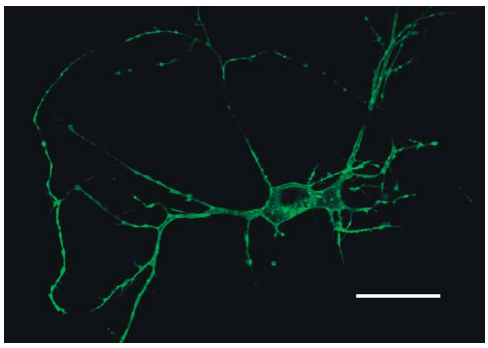

**Figure 5** Primary neurons transfected with farnesylated eGFP. Overlay of two confocal sections of eGFP-F transfected neurons from rat hippocampus. Note that the label is mainly confined to the plasma membrane, as in HEK293 cells, but considerable fluorescence is visible in the internal membranes in primary neurons. Scale bar, 50 μm.

used in voltage-clamp conditions, which may be the primary reason for the diminished signal. Increasing the DPA concentration adds capacitive load on the surface membrane, which results in aborted action potentials. Increasing the temperature alleviates this problem, however, because the kinetics of the $Na^+$ current will be faster, which should result in completion of the action potential. The measurements described here were carried out at 32 °C. Increased temperature and higher $Na^+$ channel density in neurons may allow the cells to fire even in presence of higher DPA concentrations.

The critical test for every optical detection system for neuronal activity is to record action potentials directly in a preparation from native neurons. Therefore, we transfected 7-d-old primary rat hippocampal cultures with eGFP-F DNA (**Fig. 5**). In the presence of 3-μM DPA, electrical activity and fluorescence changes were recorded from transfected neurons (**Fig. 6a**). The action potentials were resolved in the fluorescence traces with high time resolution. The mean $\Delta F/F$ of the fluorescence change of hVOS in primary neurons was 4.2% per 100 mV change and was comparable to that measured in GT-1 cells. The background instrument noise was 1%, so an action potential spike of 50 mV was easily visible (**Fig. 6b**). With decreasing spike amplitudes (25–30 mV), however, the signals were difficult to distinguish from system noise. We took the average of eight individual traces by aligning the peak of the action potential spike, which clearly improved the signal-to-noise ratio from 1.3 to 4.9 (**Fig. 6c**). Thus, small spikes should also be easily detectable in a low-noise recording system, such as in confocal spot detection or 2-photon microscopy. A histogram showing a distribution of different neuronal spikes versus the measured signal over background fluorescence revealed that in 70% of the measured signals, the $\Delta F/F$ was within 3–6% per 100 mV change in potential (**Fig. 6d**).

### A modified hVOS with fluorescently labeled antibody

The hVOS system described here is not restricted to the combination of DPA with eGFP-F. In fact, any immobile membrane-anchored molecule whose emission spectrum overlaps with DPA absorption can be used as an energy transfer donor to DPA. Whereas eGFP-F has to be expressed using cell-specific promoters, cell-specific membrane antibodies are readily available for many neuronal cell types. We transfected HEK293 cells with CD8 and labeled them with anti-CD8 antibody conjugated to Alexa488. The distribution of the fluorescent antibody in the HEK293 cells shows surface labeling as well as some internal labeling, as would be expected when the antibody recycles to internal compartments (**Fig. 7a**). Voltage change ranging from −200 mV to 100 mV (from a holding potential of −150 mV) causes a fast fluorescence signal that correlates with translocation of DPA (**Fig. 7b**). The steady-state fluorescence voltage relationship (**Fig. 7c**) could be fitted to a single Boltzmann curve with $V_{1/2} = -51$ mV and $z = 0.58$. The smaller fractional fluorescence changes ($\Delta F/F = 1.3\%$ per 100 mV) may be due to the longer distance between DPA and the antibody compared to the DPA/eGFP-F pair. As FRET has a nonlinear dependence on distance, an energy transfer pair at distances much larger than $R_0$ will not show any distance-dependent fluorescence change.

A possible advantage of using a fluorescent antibody is that one is not restricted to genetically encoded dyes. The fluorescence readout can easily be tuned to measure at a different wavelength, for different color-coded antibodies (**Fig. 7a**,**b**) against cell-specific molecules. For example, the DPA absorption spectrum also has a significant overlap with red emission ($R_0 = 20$ Å), so red-labeled antibodies as well as red-shifted GFP derivatives can also be used to monitor membrane potential changes. The activity of identified subpopulations of cells within a single neuronal circuit can thus be monitored.

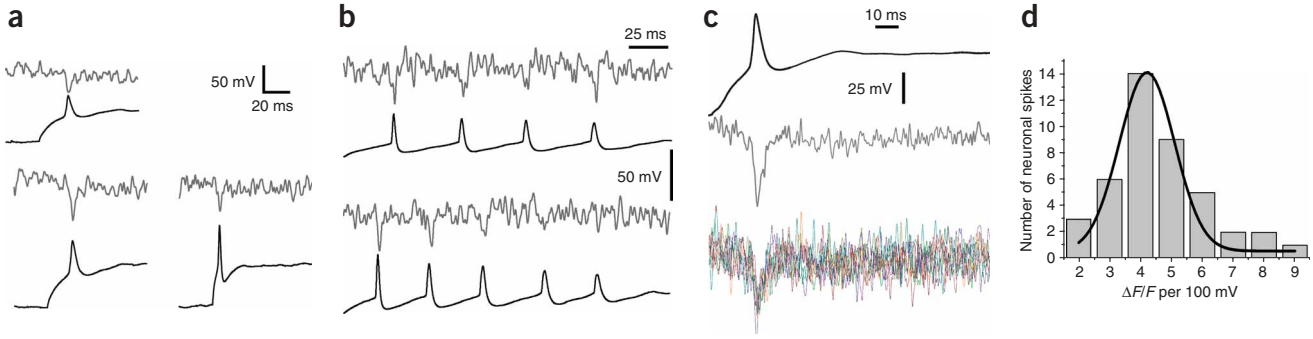


**Figure 6** Optical recordings of electrical activity in primary neuronal cultures. Electrical and optical activity was recorded from primary neuronal cultures derived from rat hippocampus. The neurons were transfected with eGFP-F and the recordings were done under current-clamp conditions in the presence of 3-μM DPA at 32 °C. (**a**) Optical response of the hVOS system to single action potentials elicited by current injection (gray, optical response; black, voltage). The fluorescence was filtered at 250 Hz. (**b**) Optical response of the hVOS system to a series of spontaneous action potentials (colors and filter as in **a**). (**c**) Averaging single sweeps improve the signal-to-noise ratio. Optical response of the hVOS system to eight individual action potentials filtered at 500 Hz (lower traces) and the averaged optical response (center trace, blue). The corresponding voltage spike is shown in red. Note that the second subthreshold depolarization is detectable in the optical recordings. (**d**) Distribution of the normalized fluorescence change per 100 mV ($n = 42$, $\Delta F/F$ (mean) = 4.2% per 100 mV, s.d. = 1.8).

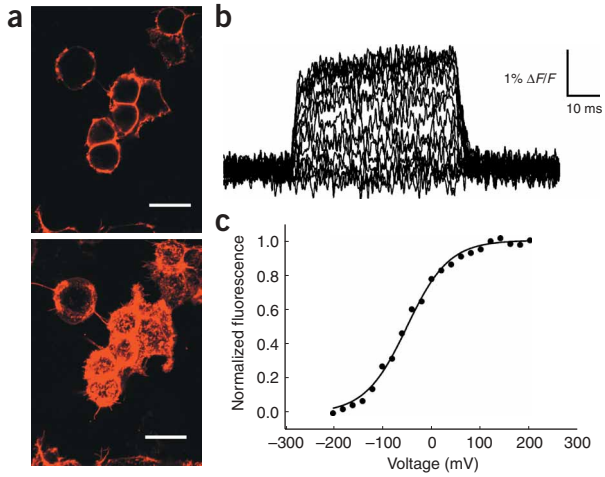


**Figure 7** Fluorescence recordings of membrane potential using DPA in conjunction with fluorescently labeled anti-CD8 antibodies. (**a**) Confocal section through CD8-expressing HEK293 cell culture labeled with anti-CD8-Alexa647 antibody. Scale bars, 20 μm. (**b**) Fluorescence response of CD8-expressing HEK293 cells labeled with anti-CD8-Alexa488 in the presence of DPA. Cells were pulsed from −150 mV to potentials ranging from −200 mV to +100 mV in steps of 20 mV. The fluorescence was filtered at 5 kHz. The data shown are single sweeps. (**c**) Fluorescence voltage characteristics for the data shown in **b**. The data were fitted to a single-component Boltzmann curve, with $V_{1/2} = -51$ mV and $z = 0.58$.

## DISCUSSION

In order to image electrical activity in neurons, a putative genetically encoded voltage-sensing fluorescent probe has to fulfill several requirements. The probe should not only have a fast response time, but it should also have a short refractory period and a large linear fluorescence response, especially in the voltage range of a typical action potential. And finally, at working concentrations, the probe components must not be toxic to the organism or tissue under investigation.

The hybrid approach combining a genetically encoded fluorescent reporter protein (eGFP-F) with a synthetic voltage-sensing molecule fulfils many of the above criteria. The hVOS system shows robust fluorescence changes up to 34% $\Delta F/F$ per 100 mV with an apparent valence of $0.5e_0$ estimated from Boltzmann fits to the fluorescence-voltage relationship. As a result of the shallow fluorescence voltage curves, the hVOS system has a large dynamic range (−150 to +50 mV), which spans the entire voltage range seen during neuronal activity. The response time constant of the hVOS system is 0.53 ms, which is sufficiently fast to record repetitive electrical activity in neuronal populations (**Fig. 6**). Although the use of a nonfluorescent acceptor like DPA does not allow measurements in ratiometric mode, there are a number of advantages to estimating voltage change by monitoring just donor fluorescence (see **Supplementary Note**). These include low background fluorescence due to the lack of direct excitation of the acceptor and the choice of a wide range of chromophores to optimize the magnitude of the signal. Furthermore, the actual gain in signal-to-noise ratios due to ratiometric measurements for FRET change are seen only in a limited range of conditions (**Supplementary Note**).

The use of DPA as a permeable ion may raise the concern that it could influence the membrane potential. Previously it has been shown that 1-h incubation in the presence of 10-μM DPA does not affect the resting membrane potential of the squid giant axon[18]. The contribution of a permeable ion to the equilibrium potential can be calculated using the Goldman-Hodgkin-Katz equation using its permeability and activity. The relative permeability coefficient of DPA with respect to potassium ($P_{DPA}/P_K$) is estimated to be 100. At 5 μM DPA, its contribution to the equilibrium resting potential is less than 2 mV. Thus, at concentrations used for optical measurements, the DPA does not shift the equilibrium potentials significantly. Nevertheless, the addition of DPA increases the capacitive load on the membranes, which may lead to abortive firing or subthreshold activity in the neurons. The calculated increase in membrane charge is $8{,}300e_0$ (DPA molecules) per μm$^2$ at a concentration of 2 μM, which corresponds to a 70% increase in membrane capacitance. It is worth noting that a similar increase in membrane capacitance is also produced by ion channel–based voltage indicators. In this case, every ion channel that inserts into the membrane adds up to $12–13e_0$, compared to $1e_0$ for each DPA molecule. A typical expression level of voltage-sensitive ion channels used in previous demonstrations of genetically encoded probes adds approximately 23,000 charges per μm$^2$—a threefold larger charge per unit area than that produced by DPA[22]. More pertinently, the capacitive load added to the membrane by the charged DPA molecules is minimized because of its shallow voltage dependence, which distributes the charge movement over a 150-mV voltage range. In comparison, most of the charges in an ion channel move over a 40-mV voltage range, adding a substantial capacitive load close to the threshold of an action potential. Recordings of field potentials in hippocampal slices (at 35 °C) indicate that the effect of increased capacitance (or some unknown toxicity) is manifested only at concentrations five times higher than those used to measure action potential spikes in neurons.

### The genetic versus hybrid approach to voltage sensing

The hybrid approach, which combines genetic and synthetic components, represents a major departure in probe design compared to other protein-based voltage probes. The performance of the hybrid system compares favorably with other genetically encoded voltage probes (**Table 1**). Previous genetically encoded fluorescent voltage sensors were based on the voltage sensor of voltage-sensitive ion channels. VSFP1 and hVOS both cover the entire membrane potential range of neuronal activity. In contrast, FlaSH and SPARC have steep voltage dependencies, which will result in a digital response upon crossing a threshold, thus being especially useful to amplify small signals. The large dynamic range seen in VSFP1 and in hVOS, on the other hand, enables quantification of the size of voltage response. Most importantly, using the hybrid approach, we were able to optically measure an action potential in a neuron using a genetically encoded probe.

Another important reason for the increased fluorescence response of the hybrid system compared to the other genetically encoded probes may be the use of farnesylated GFP. For a typical transmembrane protein, the surface-to-internal distribution is 40–60% on the surface[23]. Therefore, any GFP-fused transmembrane protein will significantly contribute to background fluorescence owing to the proteins recycling through internal membranes which do not see any membrane potential changes. eGFP-F, on the other hand, is synthesized as a soluble protein and is post-translationally modified by farnesyl and palmitoyl transferase enzymes. As a result, most of the eGFP-F remains primarily localized in the plasma membrane (**Fig. 1c**) where it contributes to optical readouts of the membrane potential.

### Outlook

The real power of genetically encoded fluorescent voltage sensors is the possibility of imaging from a specific population of neurons by expressing the eGFP-F molecule under the control of a cell-specific promoter. Various proteins, including GFP constructs, have been

successfully expressed in specific types of neurons[24,25]. An alternative approach would be to use fluorescently labeled antibodies instead of eGFP-F against cell-specific markers, as demonstrated here using antibody to CD8. Though the larger distance to the membrane reduces the size of the signals, the use of readily available antibodies might save a lot of effort. In summary, the hybrid approach reported here appears to be a promising step forward in our quest to image electrical activity from specific neuronal populations, and it opens the door to an new generation of genetically encoded probes.

## METHODS

**Chemicals and solutions.** All chemicals were purchased from Sigma-Aldrich or VWR if not stated otherwise.

The external solution for HEK293 cells consisted of 158 mM NaCl, 20 mM HEPES, 3 mM KCl and 1 mM $CaCl_2$, with pH adjusted to 7.4 with NaOH. The internal solution contained 135 mM KCl, 20 mM KF, 20 mM Hepes, 3 mM NaCl, 1 mM $MgCl_2$ and 2 mM EGTA, with pH adjusted to 7.4 with KOH. For current-clamp measurements in GT1 cells, the external solution contained 126 mM NaCl, 10 mM glucose, 2 mM $MgCl_2$, 2 mM $CaCl_2$, 2.5 mM KCl, 1.25 mM $NaH_2PO_4$ (pH adjusted to 7.2 with NaOH); the internal solution contained 120 mM $KMeSO_4$, 10 mM KCl, 5 mM NaCl, 10 mM Hepes, 2 mM $MgCl_2$, 0.1 mM EGTA, 2 mM Mg-ATP and 0.5 mM Na-GTP (pH adjusted to 7.2 with KOH).

**Molecular biology.** The pEGFP-F vector was purchased from Clontech, then it was amplified and used without further modification. The vector includes an eGFP containing the 20-amino acid farnesylation signal from the c-Ha-Ras protein, targeting the eGFP to the plasma membrane[15]. A phi-H3 vector containing CD8 at the XhoI site was transiently transfected in HEK293 cells for the anti-CD8 antibody experiments.

**Cell culture and transfection.** HEK293 cells were cultured following standard protocols in DMEM supplemented with 10% FBS, 100 U/ml penicillin and 100 μg/ml streptomycin at 37 °C and 5% $CO_2$. GT1 cells were cultured using DMEM/F12 (containing equal proportions of DMEM and Ham's F12) supplemented with 10% FBS, 5% horse serum, 100 U/ml penicillin and 100 μg/ml streptomycin at 37 °C and 5% $CO_2$.

Twelve hours before transfection, the cells were seeded on the coverslip of the recording chamber ($\phi$ = 10 mm) in a density of $10^5$ cells per chamber. The chamber was prepared by drilling a hole in the middle of a 35-mm Petri dish and gluing a No.1 coverslip onto the hole. The coverslip was subsequently treated with poly-L-lysine and laminin (both from Sigma-Aldrich). The cells were transfected with 0.2–0.5 μg DNA mixed with 1 μl of Lipofectamine 2000 (Invitrogen) using standard procedures.

Primary hippocampal neurons were cultured from newborn rat pups on Matrigel-covered coverslips as previously described[26]. After 7–10 days *in vitro*, neurons were transfected using calcium phosphate and imaged 12–48 h afterwards.

**Hippocampal slice recordings.** Coronal hippocampal slices were obtained from adult C57Bl6 mice using standard techniques[27]. Briefly, mice were anesthetized with halothane and decapitated. The brains were cooled to 4 °C then rapidly removed, and whole brain slices (350 μm thick) were cut in the horizontal plane on a VT100S vibroslicer (Leica Microsystems). Slices were incubated in artificial cerebrospinal fluid (ACSF: 126 mM NaCl, 2.5 mM KCl, 1.25 mM $NaH_2PO_4$, 2.0 mM $CaCl_2$, 2.0 mM $MgCl_2$, 26 mM $NaHCO_3$ and 10 mM D-glucose) for at least 1 h in a storage chamber at 32 °C and were then transferred to a recording chamber and continually perfused with the latter ACSF (2 ml/min, 35 °C) in an atmosphere of humidified 95% $O_2$ and 5% $CO_2$ Extracellular field excitatory postsynaptic potentials (fEPSPs) and population spikes were recorded as previously described[28] in the CA1 pyramidal cell layer following stimulation in the stratum radiatum.

**Antibody labeling.** For antibody binding, cells were incubated for 30 min in PBS with 5% donkey serum, and then for 2 h in PBS with 0.5% donkey serum and 1 μg/ml anti-CD8 Alexa488 antibody at 4 °C under steady shaking. The cells were washed twice in PBS to remove excess antibody.

**Electrophysiology, optical recordings and data analysis.** The simultaneous optical and electrophysiological recordings were performed on a setup described earlier[29], with a few small modifications. A standard patch-clamp setup was mounted on an inverted microscope (Zeiss IM35). The fluorescence was excited using a blue (470-nm) LED (Lumileds) or a mercury lamp with a low-noise power supply. The light was focused so that the light excites only one cell. The excitation light as well as the collected fluorescence were filtered using a FITC filter set (Ex: HQ480/40x; Di: Q505LP; Em: HQ535/50m, Chroma Technology). The light was collected using a high oil-immersion objective (NA 1.25, Olympus) and detected by a Photomax 200 amplifier (Dagan) with a cooled APD detector headstage. The data were acquired and stored on a PC using software developed in house.

Trains of voltage pulses of different duration and frequency were generated by a function generator, and could be added via a simple circuitry to the command voltage during the duration of a TTL signal given by the recording software.

The frequency response curve was fitted to a 4-pole low-pass filter with a corner frequency of 0.67 kHz:

$$A(f) = A_0 \Big/ \left(1 + \left(\frac{f}{f_C}\right)^{2n}\right)^{1/2}$$

with $A_0 = 0.19$, the steady state normalized fluorescence change; $f$ = applied frequency; $f_C = 0.67$ kHz, the corner frequency of the filter; and $n = 4$, order of the filter.

All experiments were done in whole-cell patch-clamp configuration. For the measurements of the action potentials, we switched to current-clamp after establishing the whole cell patch. Voltage and current protocols were applied as indicated. A 20-mM stock solution of DPA in DMSO was prepared fresh from powder every day and diluted to a final concentration of either 2 μM or 6 μM in the external recording solution. Incorporation of DPA into the membrane was monitored by observing the increase in the capacitive transient.

Electrophysiology and fluorescence data were acquired as described previously[29]. Data were analyzed using in-house analysis software, Excel (Microsoft) and Origin (Microcal).

**Confocal imaging.** Confocal images of the cells expressing eGFP-F or CD8, labeled with anti-CD8, were imaged using a commercial confocal microscope (Olympus Fluoview/IX70). Series of sections through the cells along the optical axis were recorded, to show the distribution of the fluorescence in the cell. The cells were prepared as they were for electrophysiological recordings.

*Note: Supplementary information is available on the Nature Neuroscience website.*


### ACKNOWLEDGMENTS

We thank W. Hubbell (UCLA) for the gift of DPA and A. Charles (UCLA) for the GT1 cells. Thanks to F. Chow for her assistance with primary neuronal cultures and transfections. We also thank T. Otis and M. Pratap for preparing viruses for slice transfections and for access to their setup. This work was supported by grants from the US National Institutes of Health (GM30376 to F.B., NS30549 to I.M., NS41317 to F.E.S.), the American Heart Association (0225006Y and 0535214N to B.C.) and Deutschen Forschungsgemeinschaft (BL538-1/1 to R.B.).


### COMPETING INTERESTS STATEMENT

The authors declare that they have no competing financial interests.

Published online at http://www.nature.com/natureneuroscience/
Reprints and permissions information is available online at http://npg.nature.com/reprintsandpermissions/


1. Salzberg, B.M., Grinvald, A., Cohen, L.B., Davila, H.V. & Ross, W.N. Optical recording of neuronal activity in an invertebrate central nervous system: simultaneous monitoring of several neurons. *J. Neurophysiol.* **40**, 1281–1291 (1977).
2. Djurisic, M. *et al.* Optical monitoring of neural activity using voltage-sensitive dyes. *Methods Enzymol.* **361**, 423–451 (2003).
3. Ikegaya, Y. *et al.* Synfire chains and cortical songs: temporal modules of cortical activity. *Science* **304**, 559–564 (2004).
4. Lieke, E.E., Frostig, R.D., Arieli, A., Ts'o, D.Y., Hildesheim, R. & Grinvald, A. Optical imaging of cortical activity: real-time imaging using extrinsic dye-signals and high resolution imaging based on slow intrinsic-signals. *Annu. Rev. Physiol.* **51**, 543–559 (1989).

5. Grinvald, A., Salzberg, B.M., Lev-Ram, V. & Hildesheim, R. Optical recording of synaptic potentials from processes of single neurons using intracellular potentiometric dyes. *Biophys. J.* **51**, 643–651 (1987).
6. Miyawaki, A. Fluorescence imaging of physiological activity in complex systems using GFP-based probes. *Curr. Opin. Neurobiol.* **13**, 591–596 (2003).
7. Miesenbock, G. Genetic methods for illuminating the function of neural circuits. *Curr. Opin. Neurobiol.* **14**, 395–402 (2004).
8. Siegel, M.S. & Isacoff, E.Y. A genetically encoded optical probe of membrane voltage. *Neuron* **19**, 735–741 (1997).
9. Ataka, K. & Pieribone, V.A. A genetically targetable fluorescent probe of channel gating with rapid kinetics. *Biophys. J.* **82**, 509–516 (2002).
10. Sakai, R., Repunte-Canonigo, V., Raj, C.D. & Knopfel, T. Design and characterization of a DNA-encoded, voltage-sensitive fluorescent protein. *Eur. J. Neurosci.* **13**, 2314–2318 (2001).
11. Gonzalez, J.E. & Tsien, R.Y. Voltage sensing by fluorescence resonance energy transfer in single cells. *Biophys. J.* **69**, 1272–1280 (1995).
12. Cacciatore, T.W. *et al.* Identification of neural circuits by imaging coherent electrical activity with FRET-based dyes. *Neuron* **23**, 449–459 (1999).
13. Bedlack, R.S., Jr., Wei, M.D., Fox, S.H., Gross, E. & Loew, L.M. Distinct electric potentials in soma and neurite membranes. *Neuron* **13**, 1187–1193 (1994).
14. Rohr, S. & Salzberg, B.M. Multiple site optical recording of transmembrane voltage (MSORTV) in patterned growth heart cell cultures: assessing electrical behavior, with microsecond resolution, on a cellular and subcellular scale. *Biophys. J.* **67**, 1301–1315 (1994).
15. Jiang, W. & Hunter, T. Analysis of cell-cycle profiles in transfected cells using a membrane-targeted GFP. *Biotechniques* **24**, 349–354 (1998).
16. Loew, L.M. *et al.* A naphthyl analog of the aminostyryl pyridinium class of potentiometric membrane dyes shows consistent sensitivity in a variety of tissue, cell, and model membrane preparations. *J. Membr. Biol.* **130**, 1–10 (1992).
17. Chanda, B., Asamoah, O.K., Blunck, R., Roux, B. & Bezanilla, F. Gating charge displacement in voltage-gated ion channels involves limited transmembrane movement. *Nature* **436**, 852–856 (2005).
18. Fernandez, J.M., Taylor, R.E. & Bezanilla, F. Induced capacitance in the squid giant axon. Lipophilic ion displacement currents. *J. Gen. Physiol.* **82**, 331–346 (1983).
19. de Ruyter van Steveninck , RR., Lewen, G.D., Strong, S.P., Koberle, R. & Bialek, W. Reproducibility and variability in neural spike trains. *Science* **275**, 1805–1808 (1997).
20. Kalyanaraman, B., Feix, J.B., Sieber, F., Thomas, J.P. & Girotti, A.W. Photodynamic action of merocyanine 540 on artificial and natural cell membranes: involvement of singlet molecular oxygen. *Proc. Natl. Acad. Sci. USA* **84**, 2999–3003 (1987).
21. Hales, T.G., Sanderson, M.J. & Charles, A.C. GABA has excitatory actions on GnRH-secreting immortalized hypothalamic (GT1–7) neurons. *Neuroendocrinology* **59**, 297–308 (1994).
22. Bezanilla, F., Perozo, E. & : Stefani, E. Gating of Shaker $K^+$ channels: II. The components of gating currents and a model of channel activation. *Biophys. J.* **66**, 1011–1021 (1994).
23. Salter-Cid, L. *et al.* Transferrin receptor is negatively modulated by the hemochromatosis protein HFE: implications for cellular iron homeostasis. *Proc. Natl. Acad. Sci. USA* **96**, 5434–5439 (1999).
24. Metzger, F. *et al.* Transgenic mice expressing a pH and Cl- sensing yellow-fluorescent protein under the control of a potassium channel promoter. *Eur. J. Neurosci.* **15**, 40–50 (2002).
25. Oliva, A.A., Jr., Jiang, M., Lam, T., Smith, K.L. & Swann, J.W. Novel hippocampal interneuronal subtypes identified using transgenic mice that express green fluorescent protein in GABAergic interneurons. *J. Neurosci.* **20**, 3354–3368 (2000).
26. Sippy, T., Cruz-Martin, A., Jeromin, A. & Schweizer, F.E. Acute changes in short-term plasticity at synapses with elevated levels of neuronal calcium sensor-1. *Nat. Neurosci.* **6**, 1031–1038 (2003).
27. Gordey, M., Mekmanee, L. & Mody, I. Altered effects of ethanol in NR2A(DeltaC/DeltaC) mice expressing C-terminally truncated NR2A subunit of NMDA receptor. *Neuroscience* **105**, 987–997 (2001).
28. Stell, B.M., Brickley, S.G., Tang, C.Y., Farrant, M. & Mody, I. Neuroactive steroids reduce neuronal excitability by selectively enhancing tonic inhibition mediated by delta subunit-containing $GABA_A$ receptors. *Proc. Natl. Acad. Sci. USA* **100**, 14439–14444 (2003).
29. Blunck, R., Starace, D.M., Correa, A.M. & Bezanilla, F. Detecting rearrangements of shaker and NaChBac in real-time with fluorescence spectroscopy in patch-clamped mammalian cells. *Biophys. J.* **86**, 3966–3980 (2004).
30. Knopfel, T., Tomita, K., Shimazaki, R. & Sakai, R. Optical recordings of membrane potential using genetically targeted voltage-sensitive fluorescent proteins. *Methods* **30**, 42–48 (2003).